

Experimental study of the high strain rate shear behaviour of Ti6Al4V

Jan Peirs^a, Patricia Verleysen^b and Joris Degrieck^c

¹Department of Materials Science and Engineering, Ghent University, Technologiepark 903, 9052 Zwijnaarde (Ghent), Belgium

^aJan.Peirs@UGent.be, ^bPatricia.Verleysen@UGent.be, ^cJoris.Degrieck@UGent.be

Keywords: Ti6Al4V; Hopkinson; shear; high strain rate; DIC; finite element simulation

Abstract. Three different high strain rate shear test techniques are applied on the titanium alloy Ti6Al4V. Two techniques for testing of bulk materials and one technique for sheet materials are used: torsion of thin-walled tubes, compression of hat-shaped specimens and tension of planar shear specimens. The tests are carried out on respectively torsion, compression and tensile split Hopkinson bar setups. Although shear stresses dominate the stress state in these three tests, the local stress state and its distribution and evolution are different. Therefore, the three techniques are considered to be rather complementary than equivalent tests. In this work, the value of the three test techniques for material characterization is evaluated. Where possible, digital image correlation (DIC) is used to clarify the test results. In addition, parameters difficult to assess experimentally are estimated through finite element simulations of the three tests.

Introduction

There are many applications where metals are dynamically loaded in shear (e.g. machining, punching, impact,...). Moreover, ductile metals basically deform plastically in shear, regardless the loading mode. Therefore, shear tests are an obvious way to study the material behaviour. Furthermore, characterization of the material behaviour by shear testing yields some distinct advantages over the more frequently used uni-axial tensile and compression tests. In general, larger strains are reached in shear tests, by which better material modelling can be achieved. Besides studying the plastic material behaviour, shear tests are also useful for investigation of the fracture behaviour at low stress triaxiality, including the formation of adiabatic shear bands.

Special experimental techniques have been developed to study the high strain rate shear behaviour of metals. In this contribution, three different experimental techniques are evaluated. Two of them are for bulk materials: compression of hat-shaped specimens and high speed torsion of thin walled tubes. For planar materials, a dynamic in-plane shear specimen is developed which is loaded in a split Hopkinson tensile setup. Besides theoretical considerations and numerical simulations, the three techniques are applied on the titanium alloy Ti6Al4V. Each of the three different tests has its advantages and disadvantages which makes them suitable for specific purposes.

Ti6Al4V is chosen because of its numerous applications in aerospace industry and ballistic protection and because this material is difficult to characterize by the more classical tensile tests due to early necking. Indeed, in dynamic tensile tests the uniform elongation is limited to a few percent of plastic strain. Shear tests, on the other hand, yield useful results up to strains of more than 30%, thus providing valuable data for material modelling. Furthermore, Ti6Al4V shows an interesting shear behaviour regarding the formation of adiabatic shear bands and consequent failure.

Test results, complemented with finite element simulation results are presented after a brief introduction of the three experimental techniques. Post-mortem analysis of the specimens is carried out with optical and scanning electron microscopy (SEM). These results are mainly used to characterize the fracture surface and the evolution of micro-damage before fracture.

Experimental methods

Split Hopkinson bar setups are used to apply a dynamic load on the material sample. These setups basically consist of two aligned bars with the specimen placed in between. A tensile, compression or torsion stress wave, generated at the end of the input bar propagates along the input bar towards the specimen. This wave interacts with the specimen and is partly reflected back into the input bar and partly transmitted into the output bar. The strain histories corresponding with the loading, reflected and transmitted wave (ϵ_i , ϵ_r and ϵ_t) are measured by means of strain gauges attached on the Hopkinson bars. From those waves, the total force and deformation history of the specimen is determined, based on the principles of one-dimensional elastic-wave propagation in slender bars. Strain rates achieved with the Hopkinson technique are typically in the order of 10^3s^{-1} . Although the basic principle of the three setups is similar, the method for producing the input wave is different. For the tensile and compression setup, the input wave is generated by an ertalon impactor hitting the free end of the input bar. The amplitude and length of the input wave are basically determined by respectively the impactor speed and length. For the dynamic torsion tests, the input wave is generated by the release of a pre-stressed section of the input bar. The pre-stress is applied by twisting the clamped section with a pneumatic actuator. The stress wave is released by opening a mechanical clamp through fracture of a pneumatically overloaded, pre-notched bolt.

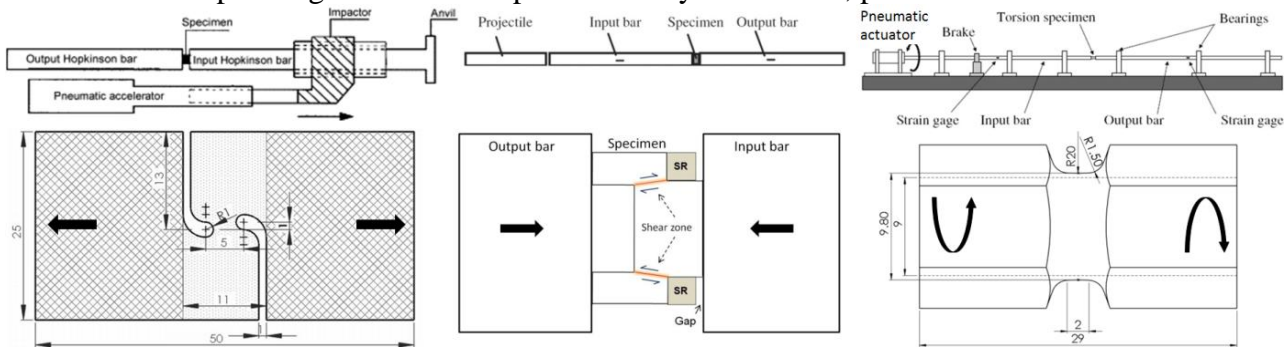


Fig. 1. Principle of the three shear tests and respective specimen geometry: planar shear test, hat-shaped specimen test and torsion test.

The three different shear test techniques with the used specimen geometries are shown in fig. 1. For sheet materials the *planar shear sample* is used. The specimen geometry is optimized by finite element simulations to obtain an almost pure shear stress state in the plastic deforming region in the Ti6Al4V specimen, even at large strains [1]. The position of the notches is an important geometrical parameter to control the stress triaxiality. In the Ti6Al4V specimen an eccentric notch position of 1mm results in the lowest stress triaxiality. The specimen cannot only be used to study the constitutive material behaviour at low and high strain rates but also for studying fracture properties at low stress triaxiality. The specimen does not require a special clamping system as is the case for the traditional simple shear test. In this way, sources of error due to inertia of the clamps, early rupture and buckling at the borders of the shear region and deformation under the clamps are avoided. The specimens used in this study are made out of a 0.6mm thick sheet with electrical discharge machining. For bulk materials the axis-symmetric *hat-shaped specimen* is used to obtain very high shear strains in a narrow zone [2]. When the hat part is pushed into the brim part, high stress and strain develops in the shear zone. The exact stress state depends on the dimensions of the hat and the brim. For the specimens used in this study and for most specimens found in literature, the diameter of the hat is slightly larger than the diameter of the brim. This is done to increase the stress and strain homogeneity in the shear zone [2] but the consequence is that no pure-shear stress state is achieved. Because the stress state is a combination of shear and compression, a very high shear strain can be reached before fracture and thus the formation of an adiabatic shear band is promoted. A stopper ring is placed around the brim to interrupt the experiment in order to avoid destruction of the shear band so that it can be studied post-mortem. Without the stopper ring, the temperature can exceed the melting temperature. Although, the specimen is suited to generate shear

bands at a known location, the complex stress distribution together with the subsurface shear zone hamper determination of stress and strain. The average stress can be estimated by the ratio of the test force and the shear surface while the strain is much more difficult to determine. Furthermore, the experimental outcome is very sensitive to geometrical variations which complicate interpretation of the experimental results. Constitutive shear stress-strain behaviour from the bulk material can accurately be obtained by *torsion tests* on *thin-walled tubular specimens*. The torsion test has several advantages: a relatively homogeneous strain distribution prevails, there are no edge effects in the circular shear zone and a pure-shear stress state is obtained. The specimen shown in fig. 1c has a gauge length L of 2mm. To ensure strain localization in the centre of the gauge section, there is a small variation in the specimen's wall thickness, following a curve with radius of 20mm with a minimum of 0.4mm. This small wall thickness is required to have sufficient through-thickness strain homogeneity.

For the specimens with visible shear zone, digital image correlation (DIC) is used to measure the local strain. Therefore, a speckle pattern is applied on the specimen surface and its deformation is recorded with a Photron APX RS high speed camera. This data is very valuable for extraction of the real material behaviour from the tests and for better understanding of the experimental results. On the other hand, for the hat-shaped specimen tests, only FE simulations and post mortem analysis can be used to study the local strain distribution because the plastic region is located subsurface.

A finite element model in ABAQUS/Explicit is made to simulate the three dynamic experiments. The strain rate and temperature dependent constitutive behaviour of Ti6Al4V is modelled with the Johnson-Cook model. The same parameters are used for the three experiments and were obtained in a previous study through tensile and planar shear tests ($A=951\text{MPa}$, $B=892\text{MPa}$, $C=0.015$, $n=0.7$, $m=0.71$, $\dot{\epsilon}=0.00008\text{s}^{-1}$) [3]. ALE adaptive meshing is used in the simulation of the hat-shaped specimen test to avoid problems due to excessive mesh distortion. The FEM is a very useful tool for enhancing the insight in the experimental results and to assess properties which are difficult to measure experimentally.

The simulated evolution of the stress triaxiality, i.e. ratio of the hydrostatic to equivalent stress, is shown in fig. 2. The triaxiality is close to 0 in the planar and torsional shear test. Thus, an almost pure-shear stress state is achieved. On the other hand, in the hat-shaped specimen the triaxiality is below $-1/3$ which implies a high hydrostatic pressure. The nucleation and growth of voids is suppressed so that very high plastic strain is obtained before fracture.

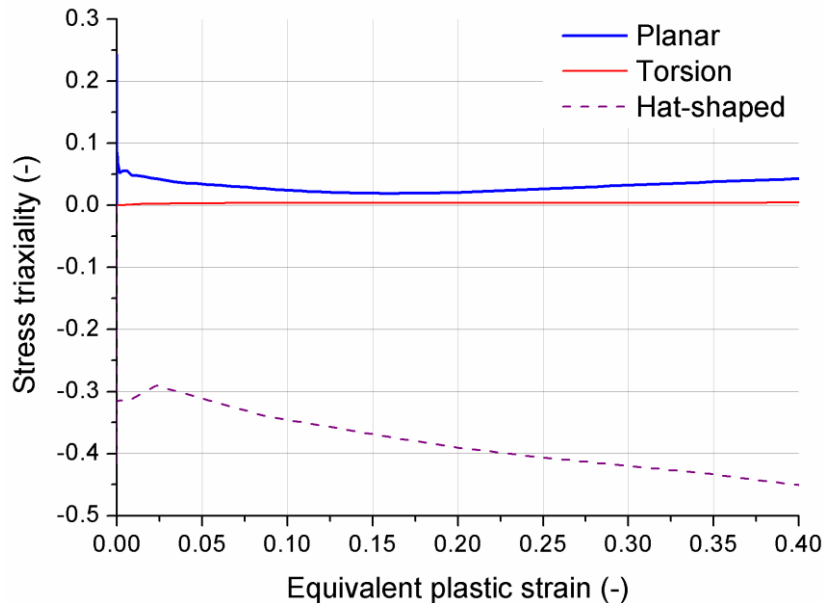


Fig. 2. Evolution of stress triaxiality in the centre of the specimen.

Experimental results

Planar shear test. Fig. 3 shows the shear stress-displacement curves of two dynamic and one static in-plane shear test. The average shear stress is calculated by dividing the total load by the shear surface area. Determination of the shear strain is not straightforward. Therefore the displacement is shown on the horizontal axis. However, an estimation of the local shear strain is made by means of DIC and FE simulation. The result is also shown on fig. 3 and the strain values are to be read on the secondary vertical axis. Unfortunately, it is not possible to measure the strain until fracture because the speckle pattern becomes too distorted for accurate DIC.

It can be seen that the yield shear stress in the dynamic tests is almost 100MPa higher than in the static test while the elongation of the specimen at fracture is less. The lower elongation in the dynamic test ($\pm 0.7\text{mm}$) is not only due to a lower fracture strain (± 0.26 vs. ± 0.4) but also because the strain is more localized which can be seen on the local shear strain curves in fig. 3. The strain localization in the dynamic tests results from thermal softening of the material. Even at the low strain rate of 0.005s^{-1} in the static test, thermal softening causes the apparent strain hardening to decrease at increasing strain values. The stress-displacement curve obtained by a finite element simulation of the planar shear tests approaches the experiment.

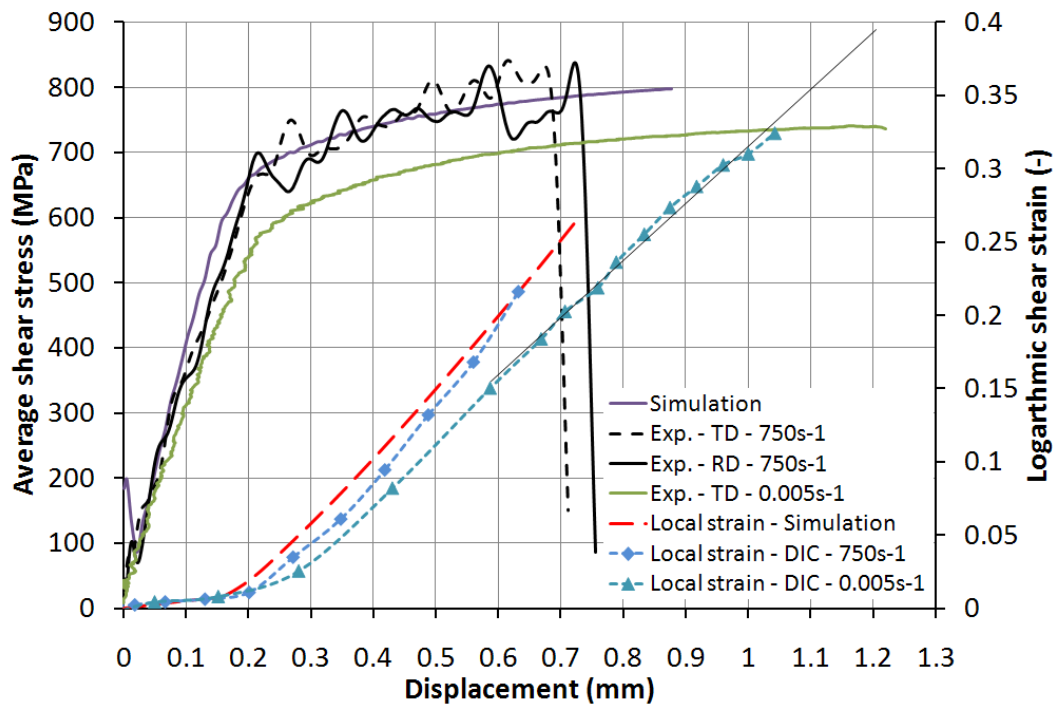


Fig. 3. Stress-displacement curve from two dynamic and one static planar shear experiment and comparison with FE simulation. Simulated and measured logarithmic strain the centre of the specimen is also shown.

Hat-shaped specimen test. Stress-displacement curves from two hat-shaped experiments are shown in fig. 4a. It is important to mention that the shear stress shown on this graph is an overestimation because it is derived from the total force on top of the specimen [2]. Although, the negative stress triaxiality in the hat-shaped specimen (fig. 2) prevents ductile fracture, all curves are characterized by a sudden drop in the force. The formation of an adiabatic shear band is catastrophic for the load carrying capacity of the material. The occurrence of adiabatic shear bands is sensitive to geometrical variations of the specimen which causes large scatter in the experimental results. From other not shown test results it was clear that the different loading speed in Exp1 (0.6m/s) and Exp2 (1.9m/s) has no clear effect on the force-displacement curves.

Two simulations of the experiment are done: with and without taking into account adiabatic heating effects. It can be seen on fig. 4a that the simulation predicts the formation of the adiabatic shear band when adiabatic heating and subsequent thermal softening is included in the model. The

shear band is formed when the thermal softening effect becomes larger than the materials strain hardening. For the JC material model parameters used in this study this happens at a logarithmic shear strain of approximately 0.70.

Fig. 4b shows a micrograph of the adiabatic shear band. The shear band has a width of only 5 μ m. Consequently, as soon as the shear band is formed, very high strains and temperatures develop. Meanwhile the microstructure of the material in the shear band evolves from large elongated grains to fragmented nano-sized grains. Finally, the shear bands' microstructure is destroyed by friction of the fracture surfaces.

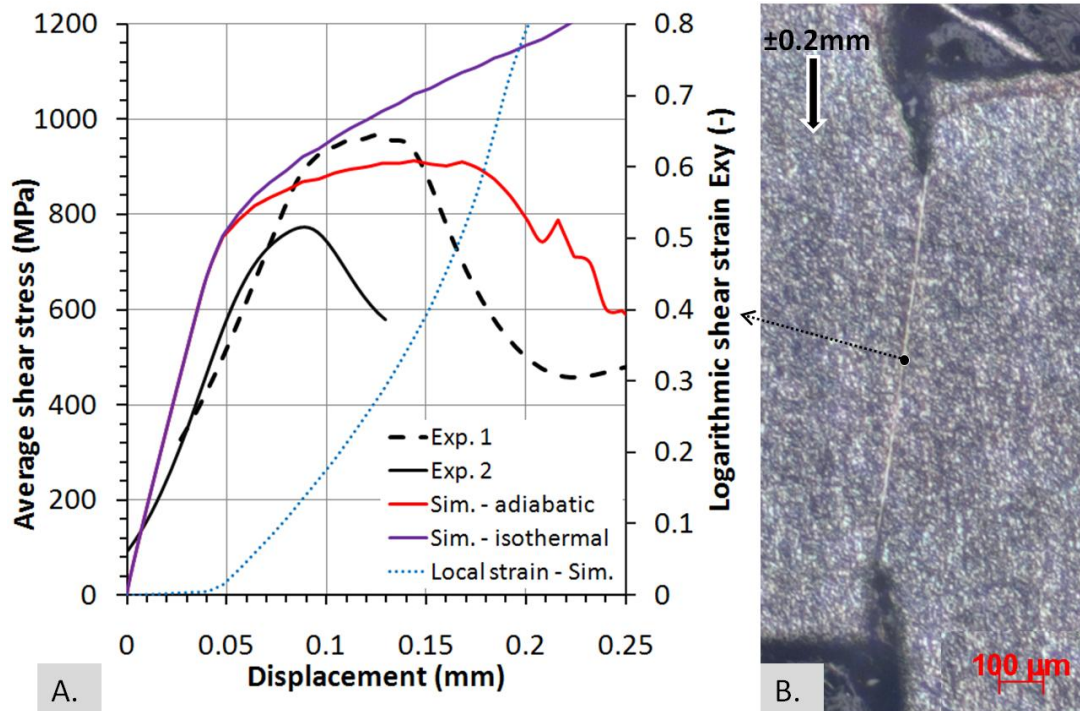


Fig. 4. A. Experimental and simulated stress-displacement curves of hat-shaped specimen experiments and local shear strain in shear band determined by FE simulation. B. Optical micrograph of shear region with shear band after 0.2mm displacement.

Torsion test. Three experimental and one simulated stress-strain curve of torsion tests are shown in fig. 5. The average shear strain γ is calculated by $r_a\theta/L$ with r_a the specimen radius, L gauge section length and θ the twist angle. The effect of the strain rate on the shear stress is not very pronounced and within experimental scatter, caused by dimensional variations of the specimen. For the FEM, a very basic failure model with critical fracture strain of 26% is added while the JC model remains identical to the model used for the planar and hat-shaped shear tests. The correspondence between the simulated and experimental stress-strain curve is satisfactory but a slight overestimation of the shear stress is made.

The figure also presents the local logarithmic shear strain E_{xy} measured at a point in the centre of the specimens' gauge section with DIC and compared with the strain in the simulation. Although, the strain is not homogeneously distributed along the gauge section, the local strain E_{xy} corresponds well with the average shear $\gamma \approx 2E_{xy}$. It can be concluded that for this particular material and specimen geometry, the stress-strain curves for the shear test are representative for the material behaviour because the error made by neglecting the strain outside the gauge section in the calculation of γ is compensated by the non-homogeneous strain distribution in the gauge section [4].

Conclusions

High strain rate shear experiments have been carried out on Ti-6Al-4V. Three different techniques have been used: tension of planar shear specimens, compression of hat-shaped specimens and torsion of thin-walled tubes. The experimental results of the torsion tests (fig. 5) and planar shear

tests are very comparable. The yield stress and maximal stress in the planar shear test is only slightly higher than in the torsion test and the maximal strains, estimated through DIC and FEM, are similar. In contrast with the planar shear test, in the torsion specimen there are no free edges confining the shear region which makes the strain distribution more homogeneous. In the hat-shaped specimen tests, adiabatic shear bands are formed before ductile fracture occurs because of the negative stress triaxiality. This feature together with the relative easiness of interrupting the experiments at a known deformation makes this technique suited for studying strain localization. For all tests on Ti-6Al-4V and in particular with hat-shaped specimens, the experimental results are affected by variations of the specimen dimensions. Accurate production of the specimens is a first requirement to successful experiments.

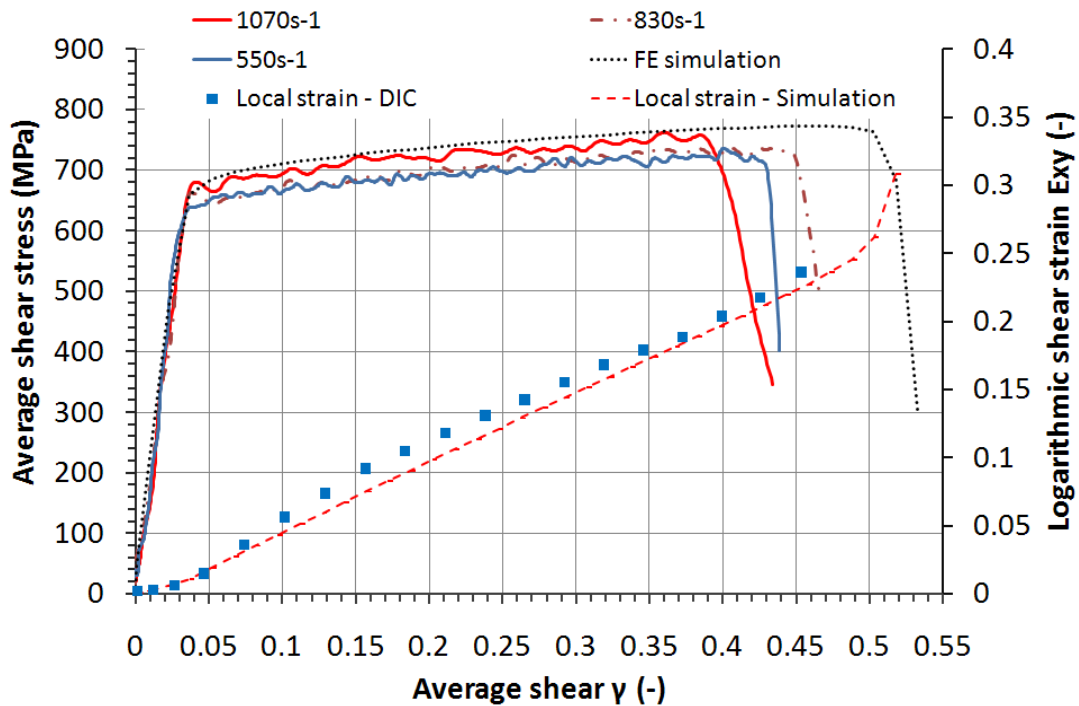


Fig. 5. Shear stress-strain curves from torsion experiments and simulation ($950s^{-1}$).

Acknowledgment

The authors would like to acknowledge The Interuniversity Attraction Poles Program (IUAP) of the Federal Science Policy of Belgium and the partners of IUAP-VI (www.m3phys.be). The authors acknowledge the technical support of Dr. P. Lava and Dr. D. Debruyne from the Catholic University College Ghent for use of their in-house developed image correlation software MatchID.

References

- [1] J. Peirs, P. Verleysen, W. Van Paepegem and J. Degrieck: presented at *Dymat 2009: 9th International Conference on the Mechanical and Physical Behaviour of Materials under Dynamic Loading, Vol 1/2*, 2009.
- [2] J. Peirs, P. Verleysen, J. Degrieck and F. Coghe: *Int J Impact Eng* Vol. 37 (2010), p. 703-714.
- [3] J. Peirs, P. Verleysen, W. Van Paepegem and J. Degrieck: presented at *ICEM14*, Poitiers, 2010.
- [4] A. Gilat, T. E. Schmidt and A. L. Walker: *Exp Mech* Vol. 49 (2009), p. 291-302.